A new benzimidazole/carbazole hybrid bipolar material for highly efficient deep-blue electrofluorescence, yellow–green electrophosphorescence, and two-color-based white OLEDs

Wen-Yi Hung,*[a] Liang-Chen Chi,[b] Wei-Jiun Chen,[a] You-Ming Chen,[b] Shu-Hua Chou[b] and Ken-Tsung Wong*[b]

Received 6th July 2010, Accepted 3rd August 2010
DOI: 10.1039/c0jm02143a

The bipolar molecule **CPhBzIm** exhibits an excellent solid state photoluminescence quantum yield (Φ_{PL} = 69%), triplet energy (E_T = 2.48 eV), and bipolar charge transport ability ($\mu_h \approx \mu_e \approx 10^{-6}$–$10^{-5}$ $cm^2\ V^{-1}\ s^{-1}$). We have used it to fabricate a non-doped deep-blue organic light emitting diode (OLED) exhibiting promising performance [η_{ext} = 3%; CIE = (0.16, 0.05)] and to serve as host material for a yellow–green phosphorescent OLED [η_{ext} = 19.2%; CIE = (0.42, 0.56)]. Exploiting these dual roles, we used **CPhBzIm** in a simple singly doped, two-color-based white OLED (η_{ext} = 7%; CIE = 0.31, 0.33).

Introduction

Organic light emitting diodes (OLEDs) attract considerable attention because of their great potential applications in flat-panel displays and lighting sources.[1] Among the three prime colors, many good red and green emitters have been developed to satisfy the practical requirements for OLEDs. In contrast, the development of deep-blue emitters that match the National Television System Committee (NTSC) standard blue with Commission Internationale de L'éclairage (CIE) coordinates of (0.14, 0.08) and high electroluminescence (EL) efficiencies remains a challenge that has attracted significant research effort.[2] A deep-blue emitter would be not only a major constituent in full-color displays but also the key element for generating white light in combination with its complementary color. Recently, a white OLED (WOLED) was fabricated through the novel concept of combining fluorescent blue emitters with phosphorescent green and/or red emitters.[3,4] Through careful control of the doping concentration of the complementary triplet emitter, this new strategy allows the efficient application of both the fluorescence from the host and the complementary phosphorescence from the triplet dopant simultaneously to give a white emission spectrum.[4] Compared with the widely reported stacked,[5] multi-emissive-layer,[3a,6] and multi-doped-layer[7] white OLEDs, this singly doped emissive layer device significantly reduces the complexity of the fabrication process, rendering this new device much more cost-effective and competitive than other contemporary display technologies. Along this line, a demand remains for the development of a material possessing a high triplet energy that can be used as both a deep-blue fluorescent emitter and a host material for phosphors.

In this paper, we report the synthesis, characterization, and various OLED applications of a new bipolar material, **CPhBzIm** (Scheme 1), comprising two *N*-phenylbenzimidazole units covalently linked to the C3 and C6 positions of carbazole. We selected carbazole as the core structure of **CPhBzIm** for the following reasons: (1) carbazole is chemically stable itself and can be easily modified at the 3, 6, or 9 positions. In addition, a phenyl group attached to the 9-position of carbazole can improve the thermal stability and impart good electro-optical properties.[8] (2) The moderately high oxidative potential of carbazole containing compounds make them promising as hole transport materials (HTM). In addition, the high triplet energy level of carbazole makes carbazole-cored materials efficient host materials for phosphors.[9] (3) Because of their planarity and rigidity, carbazole derivatives normally exhibit relatively intense luminescence, making it possible to prepare high-performance deep-blue OLEDs.[10] We adopted *N*-phenylbenzimidazole moieties as electron acceptors (A) because such derivatives usually exhibit good electron transport mobility, which has been reported to connect with electron donors (D) such as arylamine to form bipolar emitters/hosts.[11] The combination of the various structural features of the carbazole and benzimidazole units endows **CPhBzIm** with several advantageous properties: (1) deep-blue emissions with high quantum yields (Φ_{PL} = 69%, as a thin film); (2) high morphological and thermal stability [glass transition temperature (T_g) = 170 °C]; (3) bipolar carrier transport properties ($\mu_e \approx \mu_h \approx 10^{-6}$–$10^{-5}$ $cm^2\ V^{-1}\ s^{-1}$); and (4) suitable triplet energy (E_T = 2.48 eV), making it a suitable host for green phosphors. Non-doped deep-blue OLEDs incorporating **CPhBzIm** as the emitter exhibit a high value of η_{ext} of 3% with CIE coordinates of (0.16, 0.05), which are very close to the NTSC blue standard. Furthermore, **CPhBzIm** functions as an excellent host material for the yellow-green-emitting dopant $Ir(pbi)_2(acac)$,[12] providing high-performance OLEDs exhibiting CIE = (0.42, 0.56) and a high value of η_{ext} of 19.2% (62 cd A^{-1}) at 120 cd m^{-2}. The two CIE coordinates indicate that WOLEDs may be accessible by appropriate color mixing of blue light from **CPhBzIm** and yellow-green light from $Ir(pbi)_2(acac)$. Through

[a]*Institute of Optoelectronic Sciences, National Taiwan Ocean University, Keelung, 202, Taiwan. E-mail: wenhung@mail.ntou.edu.tw; Fax: +886 2 24634360; Tel: +886 2 24622192 ext. 6718*
[b]*Department of Chemistry, National Taiwan University, Taipei, 106, Taiwan. E-mail: kenwong@ntu.edu.tw; Fax: +886 2 33661667; Tel: +886 2 33661665*

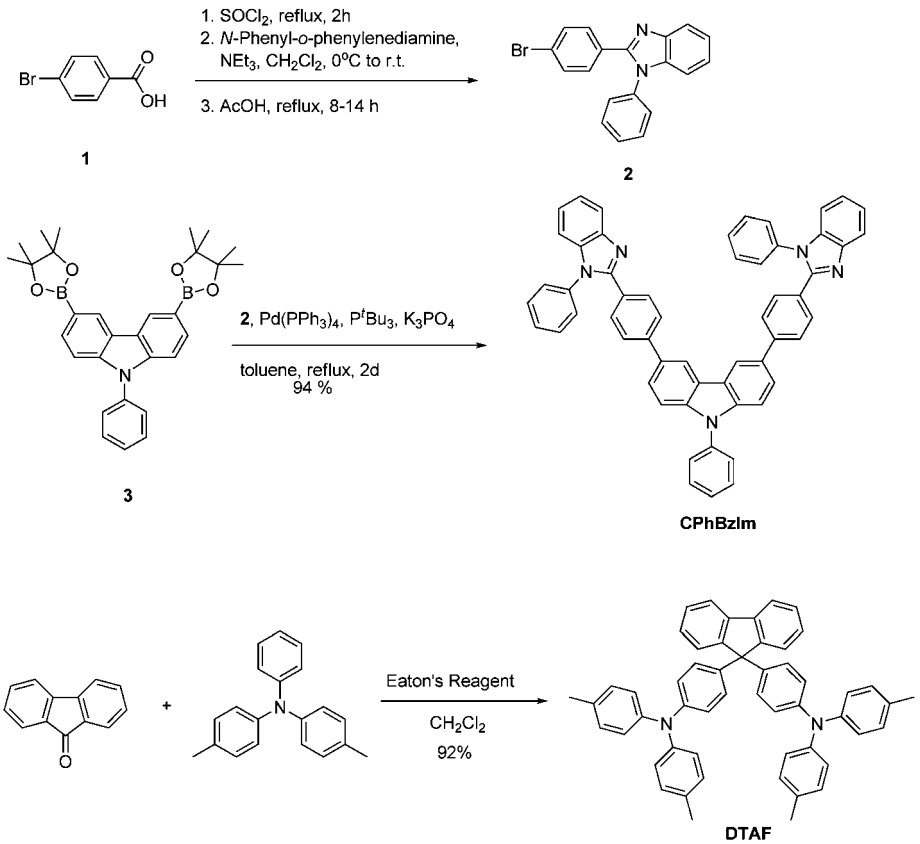

Scheme 1 Synthetic pathways toward bipolar host **CPhBzIm** and new hole-transporting material **DTAF**.

simple control over the dopant concentration (0.1 wt%), we achieved a two-color-based WOLED that exhibited EL efficiencies of 7% (15.5 cd A^{-1}) and 12.8 lm W^{-1} with CIE coordinates of (0.31, 0.33).

Results and discussion

Scheme 1 displays our synthetic route towards **CPhBzIm**. We synthesized the benzimidazole derivative **2**[13] from the reaction of *N*-phenyl-*o*-phenylenediamine with 4-bromobenzoyl chloride, which we generated from *p*-bromobenzoic acid (**1**) *in situ*. Suzuki coupling of 2-(4-bromophenyl)-1-phenylbenzimidazole (**2**) and the carbazole-based boronic ester **3**[14] gave **CPhBzIm** in 94% yield. A new fluorene-based hole-transporting material **DTAF** used in this work was also synthesized in an efficient way from 9-fluorenone with ditolylphenyl amine in the presence of Eaton's reagent.

The molecular configuration of **CPhBzIm** provided it with high thermal stability, as indicated by a high decomposition temperature (T_d = 480 °C, corresponding to 5% weight loss during thermogravimetric analysis) and a rather high glass-transition temperature [T_g = 170 °C, determined using differential scanning calorimetry (DSC)]. As a result, **CPhBzIm** forms homogeneous and stable amorphous films upon thermal evaporation.

Fig. 1(a) presents the UV–Vis absorption and photoluminescence (PL) spectra of **CPhBzIm** in dilute solution (CH_2Cl_2) and as a neat film on a quartz plate. The absorption

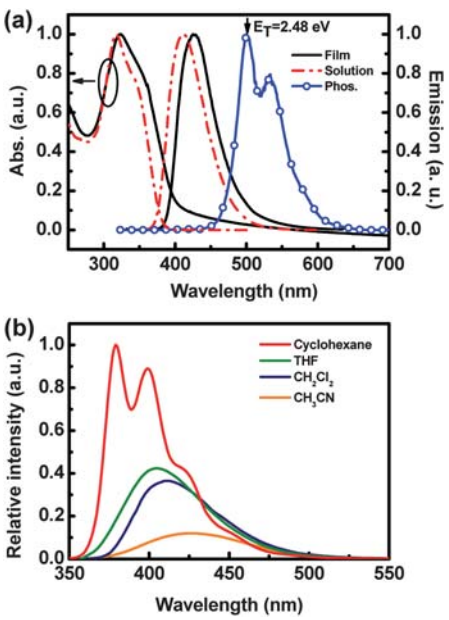

Fig. 1 (a) Room-temperature absorption (UV–Vis) and emission (PL) spectra of **CPhBzIm** in CH_2Cl_2 solutions and as neat films and the corresponding phosphorescence (Phos) spectrum recorded from an EtOH solution at 77 K. (b) The emission spectra of **CPhBzIm** in various solvents.

maximum of **CPhBzIm** in dilute solution, centered at 317 nm, is similar to that provided by its thin film (322 nm), implying that no significant intermolecular interactions occur in the ground state. However, as indicated in Fig. 1(b), the emission of **CPhBzIm** exhibits evident solvatochromism, implying the occurrence of charge transfer upon photo-excitation. To gain more insight into the electronic structure of **CPhBzIm**, density function theory (DFT) calculations were performed at a B3LYP/6-31G(d) level for the geometry optimization. As shown in Fig. 2, the HOMO of **CPhBzIm** is mainly populated over the carbazole and phenyl benzimidazole with considerable contribution from the former, whereas the LUMO has a sizable contribution from the phenyl benzimidazole fragments. Examination of the frontier orbitals of **CPhBzIm** suggests that the HOMO–LUMO excitation would shift the electron density distribution from the central carbazole to the phenyl benzimidazole moieties, leading to a polarized excited state which agrees with our observation of red-shifted emission in polar solvents.

CPhBzIm exhibits deep-blue emissions, with PL peaks centered at 412 nm in dilute solution and 426 nm in its thin film. The PL quantum yield (Φ_{PL}) of **CPhBzIm**, determined using an integrating sphere (Hamamatsu C9920), reached as high as 98% in CH_2Cl_2 and 69% in its thin film.[15] Thus, it appears that the non-coplanar conformation of **CPhBzIm** that prevents close molecular packing in the solid state also effectively inhibits excimer formation and fluorescence quenching. Such a high PL quantum yield in the solid state suggested that **CPhBzIm** could be used as an efficient deep-blue emitter in OLEDs. From the highest energy peak of the phosphorescent emission in EtOH at 77 K, we estimated the triplet energy (E_T) of **CPhBzIm** to be 2.48 eV. The extended π-conjugation, *via* 3,6-substitution on the central carbazole unit, results in **CPhBzIm** having a lower value of E_T relative to that of CzSi ($E_T = 3.02$ eV).[9a] The value of E_T of **CPhBzIm** is, however, still suitable for it to serve as a host material for green phosphorescent OLEDs (PhOLEDs).

Fig. 3 reveals the bipolar electrochemical character of **CPhBzIm**, as evidenced using cyclic voltammetry (CV). We observed one reversible oxidation potential at 1.24 V and one quasi-reversible reduction potential at −2.06 V (*vs.* Ag/AgCl). More importantly, no electropolymerization occurred during multiple cycles of CV scanning. Thus, the appending of the electron-accepting *N*-phenylbenzimidazole units onto the carbazole core renders **CPhBzIm** with promising electrochemical stability and bipolar characteristics. Using atmospheric photoelectron spectroscopy, we estimated the energy level of the highest occupied molecular orbital (HOMO) to be −5.49 eV.

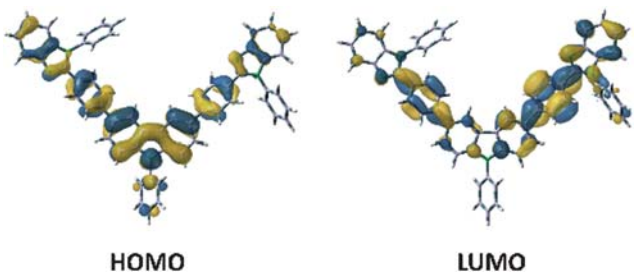

Fig. 2 Frontier molecular orbitals (HOMO and LUMO) of **CPhBzIm** calculated with DFT on a B3LYP/6-31G(d) level.

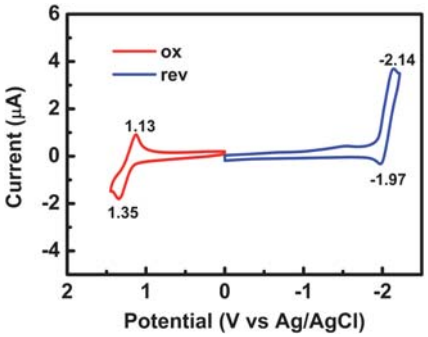

Fig. 3 Cyclic voltammogram of **CPhBzIm**.

Through subtraction of the optical energy gap ($E_g = 3.12$ eV) from the HOMO energy level, we calculated the energy level of the lowest unoccupied molecular orbital (LUMO) to be −2.37 eV.

We used the time-of-flight (TOF) transient-photocurrent technique at room temperature to determine the carrier mobilities of **CPhBzIm**. Fig. 4(a) and (b) present the representative TOF transient for holes and electrons, respectively, of **CPhBzIm**, revealing dispersive transport behavior. To determine the carrier mobilities, the carrier transit time, t_T, can be evaluated from the

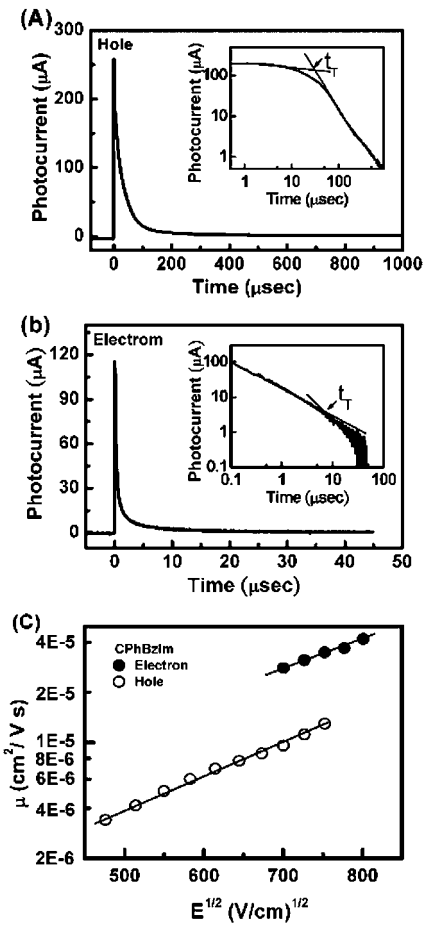

Fig. 4 Typical transient photocurrent signals for **CPhBzIm** (thickness: 1.56 μm) at $E = 5.7 \times 10^5$ V cm^{-1}: (a) hole; (b) electron. Insets: Double-logarithmic plots of (a) and (b). (c) Electron and hole mobilities plotted with respect to $E^{1/2}$.

intersection point of two asymptotes in the double-logarithmic representation of the TOF transient. Fig. 4(c) displays the field dependence of the carrier mobility of **CPhBzIm**; the hole mobility ranged from 3.4×10^{-6} to 1.3×10^{-5} cm^2 V^{-1} s^{-1} for fields varying from 2.3×10^5 to 5.7×10^5 V cm^{-1}; the electron mobility ranged from 2.8×10^{-6} to 4.2×10^{-6} cm^2 V^{-1} s^{-1} for fields varying from 4.9×10^5 to 6.4×10^5 V cm^{-1}. The ability of **CPhBzIm** to conduct both electrons and holes is important for maintaining charge balance in the emissive layer (EML), in turn generating broader recombination zones and steering the electrons and holes away from the interfaces with the charge-transport layers to suppress emissive exciton quenching.

Because of its high solid state PL quantum yield, **CPhBzIm** can be applied to fabricate non-doped deep-blue-emitting devices. In addition, the high triplet energy allows **CPhBzIm** to serve as a host material for green PhOLEDs. Hence, we fabricated devices incorporating **CPhBzIm** layers doped with various concentrations of Ir(pbi)$_2$(acac) to realize blue, yellow–green, and white light emissions from a simple three-layer configuration: indium tin oxide (ITO)/poly(3,4-ethylenedioxythiophene):poly(styrene sulfonate) (PEDOT:PSS) (30 nm)/**DTAF** (25 nm)/**CPhBzIm** doped with x% (pbi)$_2$Ir(acac) (25 nm)/TPBI (50 nm)/LiF (0.5 nm)/Al (100 nm). Here, we used DTAF as the hole-transporting layer (HTL) because it possesses an appropriate HOMO energy level (–5.22 eV) to provide a low hole injection barrier, a low-lying LUMO energy level (–1.75 eV) to block the injected electrons, and a high triplet energy level (E_T = 2.87 eV) to confine triplet excitons within the EML (see the schematic energy level diagram Fig. 5). We used the complex (pbi)$_2$Ir(acac) as the yellow-green dopant[12] and TPBI as an electron-transport and hole-blocking layer.[16]

Fig. 6 presents the current density–voltage–luminance (I–V–L) characteristics and EL efficiencies of devices prepared at various doping concentrations. When we increased the concentration of the phosphor, the hole-injection efficiency increased, presumably because of direct charge injection from the **DTAF** (HTL) into Ir(pbi)$_2$(acac). Fig. 7 displays EL spectra and CIE coordinates of these OLEDs; Table 1 summarizes the device performances. All devices displayed low turn-on voltages in the range 2–2.5 V. The non-dopant device **A** exhibited the pure blue emission [CIE (0.16, 0.05)] of **CPhBzIm**, almost matching the standard blue point recommended by the NTSC. Its maximum brightness was 4600 cd m^{-2} at 12 V; its maximum external quantum efficiency (η_{ext}) was 3%. Even at a practical brightness of 1000 cd m^{-2}, the

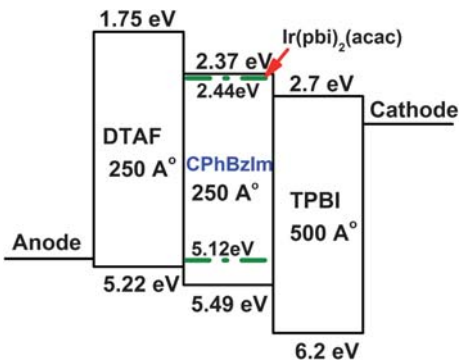

Fig. 5 Schematic energy levels diagram of device.

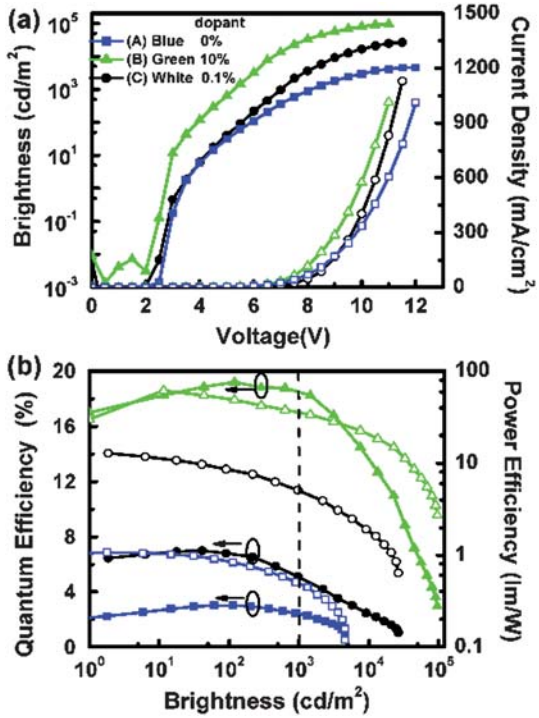

Fig. 6 (a) I–V–L characteristics and (b) EL efficiency plotted with respect to brightness for **CPhBzIm** doped with various concentrations of Ir(pbi)$_2$(acac).

performance (η_{ext}) of device **A** remained as 2.4% (8.1 V). Thus, the high PL quantum efficiency and balanced charge mobilities make **CPhBzIm** a promising candidate for realizing fairly good deep-blue light emitting devices. In device **B**, **CPhBzIm** functioned as the host for the yellow–green dopant (pbi)$_2$Ir(acac); the optimal performance occurred at a doping concentration of 10 wt%. Device **B** featured a relatively low turn-on voltage of 2 V and a maximum brightness of 96 000 cd m^{-2} at 1014 mA cm^{-2} at 11 V, with CIE coordinates of (0.42, 0.56). The maximum values of η_{ext} [19.2% (62 cd A^{-1})] and η_p (62 lm W^{-1}) were achieved at a brightness of 120 cd m^{-2}. Even at a practical brightness of 1000 cd m^{-2}, the EL efficiencies remained at 18.5% (57.4 cd A^{-1}) and 35 ml W^{-1}, with only a limited external quantum efficiency roll-off. We believe that the balanced electron and hole transporting

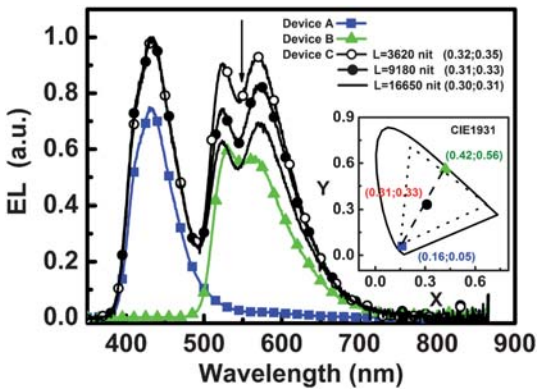

Fig. 7 EL spectra and CIE1931 coordinates of devices prepared at various doping concentrations.

Table 1 Electroluminescence data of the devices prepared at various doping concentrations

	Dopant [wt %]	V_{on}[a]/V	L_{max}/cd m^{-2}	I_{max}/mA cm^{-2}	max. η_{ext}/%	max. η_l/cd A^{-1}	max η_p/lm W^{-1}	L = 1000 cd m^{-2}[V, %]	CIE1931 [x, y]
A	0	2.5	4 600 (12 V)	1013	3	1.6	1.07	8.1, 2.4	0.16, 0.05
B	10	2	96 000 (11 V)	1014	19.2	62	62	5.2, 18.5	0.42, 0.56
C	0.1	2.5	26 500 (11.5 V)	1130	7	15.5	12.8	7, 5.1	0.31, 0.33

[a] defined as the voltage at which the EL is rapidly enhanced.

behavior of **CPhBzIm** was responsible for these excellent device characteristics.

Because the line connecting the two CIE coordinates of devices **A** and **B** passed through the white region (Fig. 7), we believed that WOLEDs would be obtained at an appropriate color mixing of the blue fluorescence from **CPhBzIm** with the complementary yellow–green phosphorescence from $(pbi)_2Ir(acac)$ dispersed in **CPhBzIm**. Indeed, controlling the doping concentration at 0.1 wt% allowed us to fabricate a two-color-based WOLED in a rather simple manner. The white-emitting device **C** exhibited a low turn-on voltage of 2.5 V and a maximum brightness of 260 500 cd m^{-2} at 1130 mA cm^{-2} at 11.5 V. Fig. 7 displays the EL spectra of device **C** recorded at various brightnesses. The relative intensity of the yellow–green emission decreased slightly when the brightness increased, leading to a slight shift in the CIE coordinates from (0.32, 0.35) at 3620 cd m^{-2} to (0.30, 0.31) at 16 650 cd m^{-2}. This color shift originated from the shifting of the recombination zone upon increasing the applied voltage and from the easier formation of high-energy excitons at higher voltage.[17] The maximum values of η_{ext} [7% (15.5 cd A^{-1})] and η_p (12.8 lm W^{-1}) were achieved at a brightness of 40 cd m^{-2}. Even at a practical brightness of 1000 cd m^{-2}, the EL efficiency remained at 5.1% at 7 V.

The structure of this WOLED device—singly doped and having a single emissive layer—is much simpler than those of widely reported stacked, multi-emissive-layer, or triple-doped WOLEDs. Our results indicate that the fabrication of efficient WOLEDs can be performed in a relatively simple and cost-effective manner.

Conclusions

We have synthesized a novel bipolar material, **CPhBzIm**, comprising two electron-accepting *N*-phenylbenzimidazole units linked to the C3 and C6 positions of an electron-donating carbazole unit. The non-coplanar conformation of **CPhBzIm** provides steric bulk, resulting in stable amorphous thin films and pronounced PL quantum efficiency. We applied **CPhBzIm** to the fabrication of non-doped deep blue-emitting devices with promising performance [η_{ext} = 3%; CIE = (0.16; 0.05)]; it also served as a host material, doped with 10 wt% of the yellow–green emitter $(pbi)_2Ir(acac)$, to realize a green PhOLED exhibiting high efficiency [η_{ext} = 19.2%; CIE = (0.42; 0.56)]. Combining the deep blue fluorescence of **CPhBzIm** with the yellow–green phosphorescence of 0.1 wt% $(pbi)_2Ir(acac)$ doped in **CPhBzIm**, we obtained an efficient WOLED device [η_{ext} = 7%; CIE = (0.31, 0.33)] that was singly doped and featured a single emissive layer. Our results pave the way toward reducing the complexity and cost of fabricating efficient OLEDs for use in displays and lighting applications.

Experimental

Synthesis

Synthesis of bipolar material CPhBzIm. A mixture of 3,6-bis(4,4,5,5-tetramethyl-1,3,2-dioxaborolan-2-yl)-9-phenyl-9*H*-carbazole (**3**)[18] (1.49 g, 3 mmol) and 2-(4-bromophenyl)-1-phenyl benzoimidazole **2**[13] (2.30 g, 6.6 mmol), $Pd(PPh_3)_4$ (173 mg, 0.15 mmol), K_3PO_4 (12 mL, 2 M), tri(*tert*-butyl)phosphine (6 mL, 0.05 M in toluene, 0.3 mmol) in toluene (30 mL) was refluxed for 2 days. After cooling to room temp., the mixture was extracted twice with CH_2Cl_2. The combined organic solution was washed with brine and dried over $MgSO_4$. The product was washed twice with hexane and methanol, affording product **CPhBzIm** as a white solid (2.2 g, 94%). mp 208–209 °C; IR (KBr) ν 3040, 2921, 2850, 2358, 2336, 1597, 1499, 1470, 1450, 1378, 1281, 811, 697 cm^{-1}; ^{1}H NMR (DMSO-d_6, 400 MHz) δ 8.81 (d, J = 1.6 Hz, 2H), 7.84–7.81 (m, 8H), 7.70–7.50 (m, 19H), 7.43 (d, J = 8.4 Hz, 2H), 7.35–7.26 (m, 4H), 7.19 (d, J = 7.2 Hz, 2H); ^{13}C NMR (CD_2Cl_2, 100 MHz) δ 152.4, 143.5, 142.7, 141.4, 137.9, 137.6, 132.6, 130.3, 130.2, 128.9, 128.7, 128.0, 127.9, 127.2, 127.1, 125.8, 124.3, 123.5, 123.1, 119.9, 119.1, 110.8, 110.7; MS (*m*/*z*, FAB$^+$) 780 (39.90); HRMS (*m*/*z*, FAB$^+$) Calcd for $C_{56}H_{37}N_5$ 779.3049, found 779.3065; Anal. Calcd. C, 86.24; H, 4.78; N, 8.98. found C, 86.01; H, 4.89; N, 8.88.

Synthesis of hole-transporting material DTAF. 9*H*-Fluoren-9-one (0.18 g, 1 mmol) and 4-methyl-*N*-phenyl-*N*-*p*-tolylaniline (683 mg, 2.5 mmol) were dissolved in dichloromethane (1 mL). Under refluxing, Eaton's reagent[19] (0.3 mL, 4 mmol) was added drop-after-drop into the solution. Then, the color of the solution changed to brown. The mixture was stirred for 12 h provided a greenish suspension. After cooling to ambient temperature, the precipitate was collected by filtration and washed several times with methanol, chloroform, and $NaOH_{(aq)}$. The crude product was collected and refluxed in CH_2Cl_2 for 30 min. The precipitate was collected to afford **DTAF** as a white solid (650 mg, 0.92 mmol, 92%). mp: 374 °C (DSC); IR (KBr) ν 3031, 2920, 2857, 1610, 1502, 1439, 1321, 1299, 1271, 831, 815, 755, 732, 723 cm^{-1}; ^{1}H NMR ($CDCl_3$, 400 MHz) δ 7.73 (d, J = 7.2 Hz, 2H), 7.42 (d, J = 7.6 Hz, 2H), 7.35–7.32 (m, 2H), 7.28–7.24 (m, 2H), 7.02–6.99 (m, 12H), 6.94 (d, J = 8.4 Hz, 8H), 6.83 (d, J = 8.8 Hz, 4H), 2.28 (s, 12H); ^{13}C NMR ($CDCl_3$, 200 MHz) δ 151.7, 146.5, 145.3, 140.0, 138.8, 132.3, 129.7, 128.7, 127.5, 127.2, 126.2, 124.5, 121.9, 120.0, 96.1, 64.4, 29.7, 20.7; MS (*m*/*z*, FAB$^+$) 872 (5.75); MS (*m*/*z*, FAB$^+$) 708 (0.09); HRMS (*m*/*z*, FAB$^+$) Calcd. for $C_{53}H_{44}N_2$ 708.3504, found 708.3510; Anal. Calcd. C, 89.79; H, 6.26; N, 3.95, found C, 89.38; H, 6.21; N, 4.34.

Photophysical measurements

Steady state spectroscopic measurements were conducted both in solution and solid films prepared by vacuum (2×10^{-6} torr) deposition on a quartz plate (1.6×1.0 cm). Absorption spectra were recorded with a U2800A spectrophotometer (Hitachi). Fluorescence spectra at 300 K and phosphorescent spectra at 77 K were measured on a Hitachi F-4500 spectrophotometer upon exciting at the absorption maxima. Quantum efficiency measurements were recorded with an integration sphere coupled with a photonic multi-channel analyzer (Hamamatsu C9920), which gave anthracene a quantum yield of 23%. The experimental values of HOMO levels were determined with a Riken AC-2 photoemission spectrometer (PES), and those of LUMO levels were estimated by subtracting the optical energy gap from the measured HOMO.

Cyclic voltammetry

The oxidation potential was determined by cyclic voltammetry (CV) in CH_2Cl_2 solution (1.0 mM) containing 0.1 M tetra-*n*-butylammonium hexafluorophosphate ($TBAPF_6$) as a supporting electrolyte at a scan rate of 100 mV s^{-1}. The reduction potential was recorded in THF solution (1.0 mM) containing 0.1 M tetra-*n*-butylammonium perchlorate ($TBAClO_4$) as a supporting electrolyte at a scan rate of 100 mV s^{-1}. A glassy carbon electrode and a platinum wire were used as the working and counter electrodes, respectively. All potentials were recorded *versus* Ag/AgCl (saturated) as a reference electrode.

Time-of-flight (TOF) mobility measurements

Carrier-transport properties were studied in vapor-deposited glasses of **CPhBzIm** by the time-of-flight (TOF) transient photocurrent technique.[20] The samples for the TOF measurement were prepared by vacuum deposition using the structure: ITO glass/**CPhBzIm** (1.56 μm)/Al (150 nm), and then placed inside a cryostat and kept under vacuum. The thickness of organic film was monitored *in situ* with a quartz crystal sensor and calibrated by a thin film thickness measurement (K-MAC ST2000). A pulsed nitrogen laser was used as the excitation light source through the transparent electrode (ITO) induced photogeneration of a thin sheet of excess carriers. Under an applied dc bias, the transient photocurrent was swept across the bulk of the organic film toward the collection electrode (Al), and then recorded with a digital storage oscilloscope. Depending on the polarity of the applied bias, selected carriers (holes or electrons) are swept across the sample with a transit time of t_T. With the applied bias V and the sample thickness D, the applied electric field E is V/D, and the carrier mobility is then given by $\mu = D/(t_T E) = D^2/(Vt_T)$, in which the carrier transit time, t_T, can be extracted from the intersection point of two asymptotes to the plateau and the tail sections in double-logarithmic plots.

OLED device fabrications

All chemicals were purified through vacuum sublimation prior to use. The OLEDs were fabricated through vacuum deposition of the materials at 10^{-6} torr onto ITO-coated glass substrates having a sheet resistance of 15 Ω sqr^{-1}. The ITO surface was cleaned ultrasonically—sequentially with acetone, methanol, and deionized water—and then it was treated with UV-ozone. A hole-injection layer of poly(3,4-ethylenedioxythiophene)-poly(4-styrenesulfonate) (PEDOT:PSS) was spin-coated onto the substrates and dried at 130 °C for 30 min to remove residual water. Organic layers were then vacuum deposited at a deposition rate of *ca.* 1–2 Å s^{-1}. Subsequently, LiF was deposited at 0.1 Å s^{-1} and then capped with Al (*ca.* 5 Å s^{-1}) through shadow masking without breaking the vacuum. The *I–V–L* characteristics of the devices were measured simultaneously using a Keithley 6430 source meter and a Keithley 6487 picoammeter equipped with a calibration Si-photodiode in a glovebox system. EL spectra were measured using a photodiode array (Ocean Optics S2000) with a spectral range from 200 to 850 nm and a resolution of 2 nm.

Acknowledgements

This study was supported financially by the National Science Council and the Ministry of Economic Affairs of Taiwan.

References

1 (*a*) C. W. Tang and S. A. VanSlyke, *Appl. Phys. Lett.*, 1987, **51**, 913; (*b*) M. A. Baldo, M. E. Thompson and S. R. Forrest, *Nature*, 2000, **403**, 750.
2 (*a*) Y.-H. Kim, H.-C. Jeong, S.-H. Kim, K. Yang and S.-K. Kwon, *Adv. Funct. Mater.*, 2005, **15**, 1799; (*b*) Y.-H. Niu, B. Chen, T.-D. Kim, M. S. Liu and A. K.-Y. Jen, *Appl. Phys. Lett.*, 2004, **85**, 5433; (*c*) Z. Q. Gao, Z. H. Li, P. F. Xia, M. S. Wong, K. W. Cheah and C. H. Chen, *Adv. Funct. Mater.*, 2007, **17**, 3194; (*d*) S. Tang, M. R. Liu, P. Lu, H. Xia, M. Li, Z. Q. Xie, F. Z. Shen, C. Gu, H. P. Wang, B. Yang and Y. Ma, *Adv. Funct. Mater.*, 2007, **17**, 2869; (*e*) T.-C. Tsai, W.-Y. Hung, L.-C. Chi, K.-T. Wong, C.-C. Hsieh and P.-T. Chou, *Org. Electron.*, 2009, **10**, 158; (*f*) C.-H. Chien, C.-K. Chen, F.-M. Hsu, C.-F. Shu, P.-T. Chou and C.-H. Lai, *Adv. Funct. Mater.*, 2009, **19**, 560.
3 (*a*) Y. Sun, N. C. Giebink, H. Kanno, B. Ma, M. E. Thompson and S. R. Forrest, *Nature*, 2006, **440**, 908; (*b*) G. Schwartz, M. Pfeiffer, S. Reineke, K. Walzer and K. Leo, *Adv. Mater.*, 2007, **19**, 3672; (*c*) H. Kanno, N. C. Giebink, Y. Sun and S. R. Forrest, *Appl. Phys. Lett.*, 2006, **89**, 023503; (*d*) J. H. Seo, J. H. Park, Y. K. Kim, J. H. Kim, G. W. Hyung, K. H. Lee and S. S. Yoon, *Appl. Phys. Lett.*, 2007, **90**, 203507; (*e*) B.-P. Yan, C. C. C. Cheung, S. C. F. Kui, H.-F. Xiang, V. A. L. Roy, S.-J. Xu and C.-M. Che, *Adv. Mater.*, 2007, **19**, 3599; (*f*) Y. H. Lee, B.-K. Ju, W. S. Jeon, J. H. Kwon, O. O. Park, J.-W. Yu and B. D. Chin, *Synth. Met.*, 2009, **159**, 325.
4 (*a*) P. Anzenbacher, Jr., V. A. Montes and S. Takizawa, *Appl. Phys. Lett.*, 2008, **93**, 163302; (*b*) Y. Tao, Q. Wang, Y. Shang, C. Yang, L. Ao, J. Qin, D. Ma and Z. Shuai, *Chem. Commun.*, 2009, 77.
5 (*a*) H. Kanno, R. J. Holmes, Y. Sun, S. Kena-Cohen and S. R. Forrest, *Adv. Mater.*, 2006, **18**, 339; (*b*) F. Guo and D. Ma, *Appl. Phys. Lett.*, 2005, **87**, 173510; (*c*) C.-C. Chang, J.-F. Chen, S.-W. Hwang and C. H. Chen, *Appl. Phys. Lett.*, 2005, **87**, 253501.
6 (*a*) Y.-S. Park, J.-W. Kang, D. M. Kang, J.-W. Park, Y.-H. Kim, S.-K. Kwon and J.-J. Kim, *Adv. Mater.*, 2008, **20**, 1957; (*b*) C.-H. Chang, K.-C. Tien, C.-C. Chen, M.-S. Lin, H.-C. Cheng, S.-H. Liu, C.-C. Wu, J.-Y. Hung, Y.-C. Chiu and Y. Chi, *Org. Electron.*, 2010, **11**, 412.
7 (*a*) J. Lee, J.-I. Lee, J. Y. Lee and H. Y. Chu, *Appl. Phys. Lett.*, 2009, **94**, 193305; (*b*) Y.-H. Niu, M. S. Liu, J.-W. Ka, J. Bardeker, M. T. Zin, R. Schofield, Y. Chi and A. K.-Y. Jen, *Adv. Mater.*, 2007, **19**, 300; (*c*) X. Yang, Z. Wang, S. Madakuni, J. Li and G. E. Jabbour, *Adv. Mater.*, 2008, **20**, 2405.
8 (*a*) K. R. J. Thomas, J. T. Lin, Y. T. Tao and C. W. Ko, *J. Am. Chem. Soc.*, 2001, **123**, 9404; (*b*) K. R. J. Thomas, J. T. Lin, Y. T. Tao and C. W. Ko, *Adv. Mater.*, 2000, **12**, 1949.

9 (*a*) M. H. Tsai, H. W. Lin, H. C. Su, T. H. Ke, C. C. Wu, F. C. Fang, Y. L. Liao, K. T. Wong and C. I. Wu, *Adv. Mater.*, 2006, **18**, 1216; (*b*) S.-J. Yeh, M.-F. Wu, C.-T. Chen, Y.-H. Song, Y. Chi, M.-H. Ho, S.-F. Hsu and C. H. Chen, *Adv. Mater.*, 2008, **17**, 285; (*c*) H. Sasabe, Y.-J. Pu, K. Nakayama and J. Kido, *Chem. Commun.*, 2009, 6655; (*d*) S.-J. Su, H. Sasabe, T. Takeda and J. Kido, *Chem. Mater.*, 2008, **20**, 1691; (*e*) S. O. Jeon, K. S. Yook, C. W. Joo and J. Y. Lee, *Adv. Funct. Mater.*, 2009, **19**, 3644.

10 (*a*) S. J. Lee, J. S. Park, K. J. Yoon, Y. I. Kim, S. H. Jin, S. K. Kang, Y. S. Gal, S. Kang, J. Y. Lee, J. W. Kang, S. H. Lee, H. D. Park and J. J. Kim, *Adv. Funct. Mater.*, 2008, **18**, 3922; (*b*) S.-L. Lin, L.-H. Chan, R.-H. Lee, M.-Y. Yen, W.-J. Kuo, C.-T. Chen and R.-J. Jeng, *Adv. Mater.*, 2008, **20**, 3947; (*c*) S. Tao, Y. Zhou, C.-S. Lee, X. Zhang and S.-T. Lee, *Chem. Mater.*, 2010, **22**, 2138; (*d*) Z. Jiang, H. Yao, Z. Liu, C. Yang, C. Zhong, J. Qin, G. Yu and Y. Liu, *Org. Lett.*, 2010, **11**, 4132.

11 (*a*) C.-H. Chen, W.-S. Huang, M.-Y. Lai, W.-C. Tsao, J. T. Lin, Y.-H. Wu, T.-H. Ke, L.-Y. Chen and C.-C. Wu, *Adv. Funct. Mater.*, 2009, **19**, 2661; (*b*) Z. Ge, T. Hayakawa, S. Ando, M. Ueda, T. Akiike, H. Miyamoto, T. Kajita and M. Kakimoto, *Chem. Mater.*, 2008, **20**, 2532; (*c*) S. Takizawa, V. A. Montes and P. Anzenbacher Jr., *Chem. Mater.*, 2009, **21**, 2452.

12 (*a*) W.-S. Huang, J. T. Lin, C.-H. Chien, Y.-T. Tao, S.-S. Sun and T.-S. Wen, *Chem. Mater.*, 2004, **16**, 2480; (*b*) W.-S. Huang, J. T. Lin and H.-C. Lin, *Org. Electron.*, 2008, **9**, 557.

13 Z. Ge, T. Hayakawa, S. Ando, M. Ueda, T. Akiike, H. Miyamoto, T. Kajita and M.-a. Kakimoto, *Adv. Funct. Mater.*, 2008, **18**, 584.

14 K.-T. Wong, T.-C. Chao, L.-C. Chi, Y.-Y. Chu, A. Balaiah, S.-F. Chiu, Y.-H. Liu and Y. Wang, *Org. Lett.*, 2006, **8**, 5033.

15 Y. Kawamura, H. Sasabe and C. Adachi, *Jpn. J. Appl. Phys.*, 2004, **43**, 7729.

16 S.-J. Yeh, M.-F. Wu, C.-T. Chen, Y.-H. Song, Y. Chi, M.-H. Ho, S.-F. Hsu and C. H. Chen, *Adv. Mater.*, 2005, **17**, 285.

17 Y. Shao and Y. Yang, *Appl. Phys. Lett.*, 2005, **86**, 073510.

18 K.-T. Wong, T.-H. Hung, T.-C. Chao and T.-I. Ho, *Tetrahedron Lett.*, 2005, **46**, 855.

19 P. E. Eaton, G. R. Carlson and J. T. Lee, *J. Org. Chem.*, 1973, **38**, 4071.

20 P. M. Borsenberger and D. S. Weiss, *Organic Photoreceptors for Imaging Systems*; Marcel Dekker, New York, 1993.